



## COMPUTATION OF TWO-COMPONENT TRANSITION RATES OF PREEQUILIBRIUM STATES

A. A. Selman, \* M. H. Jasim, \*Sh. S. Shafik

IT Unit , College of Science, University of Baghdad. Baghdad-Iraq

\*Department of Physics, College of Science, University of Baghdad .Baghdad-Iraq

### Abstract

Different transition rates of the nuclear preequilibrium states in the exciton model were numerically calculated in the present work, as well as the state density and matrix element of the nuclear interaction. The calculations were based on the two-component version of the exciton model. Some comparisons were made with earlier calculations, and the results showed a good agreement. The results were explained on the bases of the effects of the differences in the particle and hole numbers, as well as the type of the incident particle and its energy. The conclusions indicated that preequilibrium nuclear reactions induced by protons differ only by small fraction from those induced by neutrons at low exciton states. At higher exciton states with  $n > 3$ , the transitions of the types  $\lambda_{\nu}^{-}$  and  $\lambda_{\pi}^{+}$  differed significantly between neutron and proton transitions, which may indicate distinguishable nuclear reaction mechanisms.

### حساب معدلات الانتقال ثنائية المركبات للحالات قبل المتوازنة

أحمد عبد الرزاق سلمان، \*مهدي هادي جاسم، \* شفيق شاکر شفيق

وحدة تكنولوجيا المعلومات، كلية العلوم، جامعة بغداد. بغداد - العراق

\*قسم علوم الفيزياء، كلية العلوم، جامعة بغداد. بغداد - العراق

### الخلاصة

في البحث الحالي، حسبت معدلات الانتقال للحالات قبل المتوازنة في التفاعلات النووية، وكذلك كثافة الحالات النووية المنهيجة وعنصر مصفوفة التفاعل النووي. النظام المستخدم مبني على الحالة ثنائية المركبات لأنموذج الجسيمة المهيجة. أجريت بعض المقارنات مع حسابات سابقة وأوضحت النتائج تطابقاً جيداً. فسرت النتائج على أساس الفروق في التوزيع العددي للجسيمة والفجوة وتأثيرها مع تأثير نوع الجسيمة الساقطة وطاقتها. تم الاستنتاج بأن التفاعلات النووية للحالة قبل المتوازنة المحتثة بالبروتون لا تختلف سوى بجزء بسيط عن تلك التفاعلات المحتثة بالنيوترون عند حالات التهيج ذات الأعداد الواطئة. عند  $n > 3$ ، ظهر فرق واضح خصوصاً بين معدلي الانتقال  $\lambda_{\nu}^{-}$  و  $\lambda_{\pi}^{+}$  مما يشير إلى تمايز ميكانيكية التفاعل النووي عند هذه المستويات.

**Introduction**

The exciton model [1-3] is a semi-classical model that is widely used to analyze different nuclear emissions within the intermediate energy range. Unlike the one-component model, the two-component exciton model differentiates between proton and neutron states during the calculations. Some recent attempts were made in order to extend the applications of this model to include heavy ion reactions [4,5], and to enlarge the relevant energy range to few GeV's [6]. A significant physical parameter required during the exciton model calculations is the state density of the excited nuclear states,  $\omega(p, h, E)$ . Table 1 lists the symbols and abbreviations used in this paper. Similar to the well-known Hauser-Feshbach model [7], the exciton model requires the determination of the ratio of the excited state densities after nuclear emission to that before. This ratio specifies the major factor needed in calculating the emission rate,  $W(n, \mathcal{E})$ . Once this rate is calculated, a weighting procedure is required to determine the total contribution of emission from each  $n$  exciton state to the total emission. This weighting procedure is the equilibration lifetime,  $T(n, E)$ , and the latter is found from solving the master equation [8], which depends mainly on the state density as well as the transition rates between different exciton states,  $\lambda$ . Extended details of the calculation procedures are found elsewhere [9]. In this research, the transition and decay rates are to be calculated numerically and compared with earlier results. The comparisons will be made by means of the transition rates, state density and effective matrix element.

**II. Transition Rates**

There are six types of transition rates for the two-component system, namely,  $\lambda_{\pi}^+$ ,  $\lambda_{\pi}^-$ ,  $\lambda_{\nu}^+$ ,  $\lambda_{\nu}^-$ ,  $\lambda_{\pi\nu}^0$ , and  $\lambda_{\nu\pi}^0$  transitions. Usually the  $\lambda_{\pi\nu}^0$  are specified by  $\lambda_{\pi\nu}$  only and the same for  $\lambda_{\nu\pi}$ . Transitions between adjacent exciton states are caused by allowed types of transmissions, namely, those who depend on the two-body interaction.

<b>Table1: A List of symbols and abbreviations used in this work.</b>	
$A$	Mass number of the target nucleus
$A_{p,h}$	Pauli blocking energy for one-component
$A_{p_{\pi}, h_{\pi}, p_{\nu}, h_{\nu}}$	Pauli term for two-component model
$E$	Excitation energy
ESM	Equidistant Spacing Model
$f(h)$	Surface correction term
$W(n, \mathcal{E})$	Emission rate from the $n^{\text{th}}$ exciton state with emission energy, $\mathcal{E}$ .
$\Theta(x - x_0)$	The Heaviside step function
$g_o, g$	Single-particle level density (s.p.l.d.) for ground and excited states. $g_{\pi}, g_{\nu}$ correspond to the same values for proton and neutron states, respectively
$\mathcal{E}$	Emission energy
$\omega_i(p, h, E)$	State density of the system for $p$ particles, $h$ holes and excitation energy $E$ . The subscript ( $i$ ) refers to the number of components: 1 for one-component and 2 for two-component model.
$n, p, h$	Exciton, particle and hole numbers, for in the one-component model; $n=p+h$
$n_{\pi}, p_{\pi}, h_{\pi}$	Proton exciton, proton particle and proton hole numbers, in the two-component model; $n_{\pi} = p_{\pi} + h_{\pi}$
$n_{\nu}, p_{\nu}, h_{\nu}$	Neutron exciton, neutron particle and proton hole numbers, in the two-component model; $n_{\nu} = p_{\nu} + h_{\nu}$
$N, Z$	Neutron and atomic (proton) numbers
$r_o, m$	Nucleon classical radius and its effective rest mass
$\lambda_2^1$	The transition rate between two exciton states determined by the type (1) and change in the exciton number $\Delta n$ (2). The type might be proton-type transition, $\pi$ , neutron-type transition, $\nu$ , or mixed type $\pi\nu$ or $\nu\pi$ . $\Delta n$ might be +2 (+), -2 (-), or zero (0). Thus $\lambda_{\pi}^+$ means transition rates of proton with $\Delta n=+2$ .

In general, Fermi golden rule is used:

$$\lambda_{x,y} = \frac{2\pi}{\hbar} |M_{x,y}|^2 \omega_f \tag{1}$$

For a system described by the two-component model there are three types of the two-body transition rates described by the following matrices,  $|M_{\pi\pi}|^2$ ,  $|M_{\pi\nu}|^2 = |M_{\nu\pi}|^2$ , and  $|M_{\nu\nu}|^2$ , for proton-proton, neutron-proton and neutron-neutron interactions, respectively. As a rough approximation, one may assume that all these interactions are the same. In general [10],

$$|M|^2 \propto \frac{1}{E} \quad (2).$$

Dobeš and Běták gave a parameterized expressions for  $M$  as follows [11],

$$|M_{\pi\nu}|^2 = \frac{K}{A N Z E} \quad (3-a),$$

$$|M_{\nu\nu}|^2 = \frac{K}{A N^2 R E} \quad (3-b),$$

$$|M_{\pi\pi}|^2 = \frac{K}{A Z^2 R E} \quad (3-c),$$

where  $K$ =fitting parameter,  $R$ =a numerical factor that accounts for different ways of interaction between like and unlike types of particles. Its value is  $\sim 2.9-3$ . Transition rates are given by many authors and slightly differ from one paper to another. However, the most recent version due to Kalbach is given here [12],

$$\lambda_{\pi}^{+} = \frac{2\pi}{\hbar} \frac{g_{\pi}^2}{2n(n+1)} \frac{[E - A_{p_{\pi+1}, h_{\pi+1}, p_{\nu}, h_{\nu}}]^{n+1}}{[E - A_{p_{\pi}, h_{\pi}, p_{\nu}, h_{\nu}}]^{n+1}} \times \{g_{\pi} n_{\pi} |M_{\pi\pi}|^2 + 2n_{\nu} g_{\nu} |M_{\pi\nu}|^2\} f(h+1) \quad (4),$$

$$\lambda_{\pi}^{-} = \frac{2\pi}{\hbar} \frac{p_{\pi} h_{\pi}}{2} \times \{g_{\pi} (n_{\pi} - 1) |M_{\pi\pi}|^2 + 2n_{\nu} g_{\nu} |M_{\pi\nu}|^2\} f(h-1) \quad (5),$$

$$\lambda_{\pi\nu}^0 = \frac{2\pi}{\hbar} |M_{\pi\nu}|^2 \times \frac{p_{\pi} h_{\pi} g_{\nu}^2 f(h) [E - B_o(p_{\pi}, h_{\pi}, p_{\nu}, h_{\nu})]^{n+1}}{n [E - A_{p_{\pi}, h_{\pi}, p_{\nu}, h_{\nu}}]^{n+1}} \times \{2[E - B_o(p_{\pi}, h_{\pi}, p_{\nu}, h_{\nu})] + n |A_{p_{\pi}, h_{\pi}, p_{\nu}, h_{\nu}} - A_{p_{\pi-1}, h_{\pi-1}, p_{\nu}+1, h_{\nu}+1}|\} \quad (6),$$

where the modified Pauli term is:

$$B_o(p_{\pi}, h_{\pi}, p_{\nu}, h_{\nu}) = \max(A_{p_{\pi}, h_{\pi}, p_{\nu}, h_{\nu}} - A_{p_{\pi-1}, h_{\pi-1}, p_{\nu}+1, h_{\nu}+1}) \quad (7).$$

The transition rates for neutrons  $\lambda_{\nu}^{+}$ ,  $\lambda_{\nu}^{-}$  and  $\lambda_{\nu\pi}^0$  are given similarly but with the subscripts  $\pi$  and  $\nu$  interchanged.

As for the residual two-body matrix element of the interaction, one can assume that the matrix elements  $|M_{\pi\pi}|^2 = |M_{\pi\nu}|^2 = |M_{\nu\nu}|^2$  are the same for the purpose of model calculations; and if needed, one may write,

$$|M_{\nu\pi}|^2 = |M_{\pi\nu}|^2 = 3 \times |M_{\pi\pi}|^2 = 3 \times |M_{\nu\nu}|^2 \quad (8),$$

which was found from a wide variety of data [10]. Denoting the average by  $|M|^2$ ,

$$|M|^2 = \frac{K}{[A(20.9 \text{ MeV} + e)]^3} \quad (\text{MeV})^2 \quad (9),$$

$$e = E/n \quad (10-a),$$

$$K = \text{constant} = 1.08 \times 10^{+6} \quad (\text{MeV})^5 \quad (10-b).$$

The most recent formulae due to Kalbach [12] is found from experimentally evaluated transition rates, namely,

$$|M|^2 = K \frac{A}{g_o^3} \left( \frac{E}{3A} + 20.9 \right)^{-3} \quad (\text{MeV})^2 \quad (11),$$

where  $K$  here is a constant that has the value 900  $(\text{MeV})^2$  for proton-proton and 2200  $(\text{MeV})^2$  for neutron-neutron reactions.

### III. The State Density

There are many formulae used for calculating the state density numerically, of which Williams' formula is the most practical [13]. The effect of Pauli correction is applied in this type and it appears as if the magnitude of the excitation energy was lowered. This means that several states are blocked, thus their contribution in the amount of the excitation energy will decrease. A net effect will be as if  $E$  becomes  $[\bar{E}A_{p,h}(p,h,E)]$ , where  $A_{p,h}(p,h,E)$  is Pauli correction term [13],

$$\omega_2(n, E) = \frac{g_{\pi}^{n_{\pi}} g_{\nu}^{n_{\nu}} (E - A_{p_{\pi}, h_{\pi}, p_{\nu}, h_{\nu}})^{n-1}}{p_{\pi}! h_{\pi}! p_{\nu}! h_{\nu}! (n-1)!} \quad (12),$$

with the correction term given in this case by the following,

$$A_{p_{\pi}, h_{\pi}, p_{\nu}, h_{\nu}} = \frac{p_{\pi} (p_{\pi} + 1) + h_{\pi} (h_{\pi} - 3)}{4 g_{\pi}} + \frac{p_{\nu} (p_{\nu} + 1) + h_{\nu} (h_{\nu} - 3)}{4 g_{\nu}} \quad (13).$$

A symmetric formula in  $p$  and  $h$  is further given by [14],

$$\omega_2(n, E) = \frac{g_\pi^{n_\pi} g_\nu^{n_\nu} (E - A_{p_\pi, h_\pi, p_\nu, h_\nu})^{n-1}}{p_\pi! h_\pi! p_\nu! h_\nu! (n-1)!} \times \Theta(E - \alpha_{p_\pi, h_\pi, p_\nu, h_\nu}) \quad (14),$$

where the Heaviside step function is,

$$\Theta(E - \alpha_{p, h}) = \begin{cases} 0 & E - \alpha_{p, h} \leq 0 \\ 1 & E - \alpha_{p, h} > 0 \end{cases} \quad (15),$$

$$\alpha_{p_\pi, h_\pi, p_\nu, h_\nu} = \frac{p_\pi(p_\pi + 1) + h_\pi(h_\pi - 1)}{2g_\pi} + \frac{p_\nu(p_\nu + 1) + h_\nu(h_\nu - 1)}{2g_\nu} \quad (16).$$

In the present work, we used this formula in order to perform our calculations. One must note that Williams' formula is quite simple. There are many other more accurate and more complicated types of formulae used for state density calculations. For more details about state density formulae, see Ref. [9].

#### IV. Results and Discussions

The present calculations were numerically made using a library of computer codes written using Matlab language. There have been some numerical comparisons with earlier standard codes in order to maintain confidence of the present codes.

First, a simple comparison is made with the state density results as seen from figure 1.

figure 2. shows another basic comparison for  $|M|$  results. From both figures, one may conclude that the present results are in a general agreement with published work. From figure 1. it is clearly seen that the match is acceptable between the results of this work and those of Kalbach [10]. Generally, for  $p$  or  $p_\pi > 2$ , the present calculations are slightly lower than those of Kalbach, however, the results are satisfactory. Although a maximum decrement is seen of about 10% in the case of  $n=5$ , this comparison is important because from it one may compare the results of the transition rates with ease. The difference may be due to errors from data graphically taken from Ref.[10] – figure 3 therein, or from round off errors. From the results of figure 2, it can be seen that the results of this work well agree with those of Ref.[10]. The transition rates of proton-proton,

$\lambda_\pi^+$  and for  $p+^{54}\text{Fe}$  at 33 MeV are plotted in figure 3-A as a function of  $E$ , and to get a better view of the results, they are plotted again as a surface in figure 3-B, where this figure shows the relation between transition rates as a function of  $E$  and  $n$ . figure 3-C. shows the same results for  $n+^{54}\text{Fe}$  reaction at 33 MeV, which shows some change, where configuration (5,4,0,0) was less than (4,4,1,0), while (1,0,4,4) was higher than (0,0,5,4). Similar method is followed in plotting

$\lambda_\pi^-$  in figure 4-A and B,  $\lambda_\nu^+$  in figures 5-A and B,  $\lambda_\nu^-$  in figure (6-A and B),  $\lambda_{\nu\pi}$  in figures 7-A and

B, and  $\lambda_{\nu\pi}$  in figures 8-A and B, respectively as found from the set of equations, eq.(4-7) and for proton and neutron as incident particles. It can be seen clearly that in all cases the transition rates reach maxima for the maximum  $(p_\pi, h_\pi)$  pair for the type  $(\pi - x)$  with  $x$  being either proton or neutron, and the minimum transition rates occur with the  $(p_\nu, h_\nu)$  pair. The same goes for transition type  $(\nu - x)$ . Physically this is reasonable and it means that preequilibrium states with the maximum particles and holes proton-type number will suffer from higher transition, and those with minimal number will have the lowest transitions, which is a direct consequence of transition rates dependence on the state density, as seen from eqs.(4-7). The sudden drop in some values of  $\lambda_{\pi\nu}$  and  $\lambda_{\nu\pi}$  at low energies are due to the effect of the Heaviside function. In all these figures, there is an important difference in the exciton configurations. In proton induced reactions, proton particles always exist, *i.e.*, the lowest configuration is (1,0, $x$ , $x$ ) with  $x$  being any value. Similar rule goes for neutron reaction.

The only significant changes from neutron to proton transition rates are seen from the results of calculations of  $\lambda_\pi^+$  and  $\lambda_\nu^-$ , as shown from figures 4 and 6. Although in these figures the results of most configurations are the same except for (1,0,4,4) for proton and (0,0,4,5) for neutron cases. Most other cases produced the exact (~98%) transition rates when dealing with neutron or proton as incident particles with the same excitation energy.

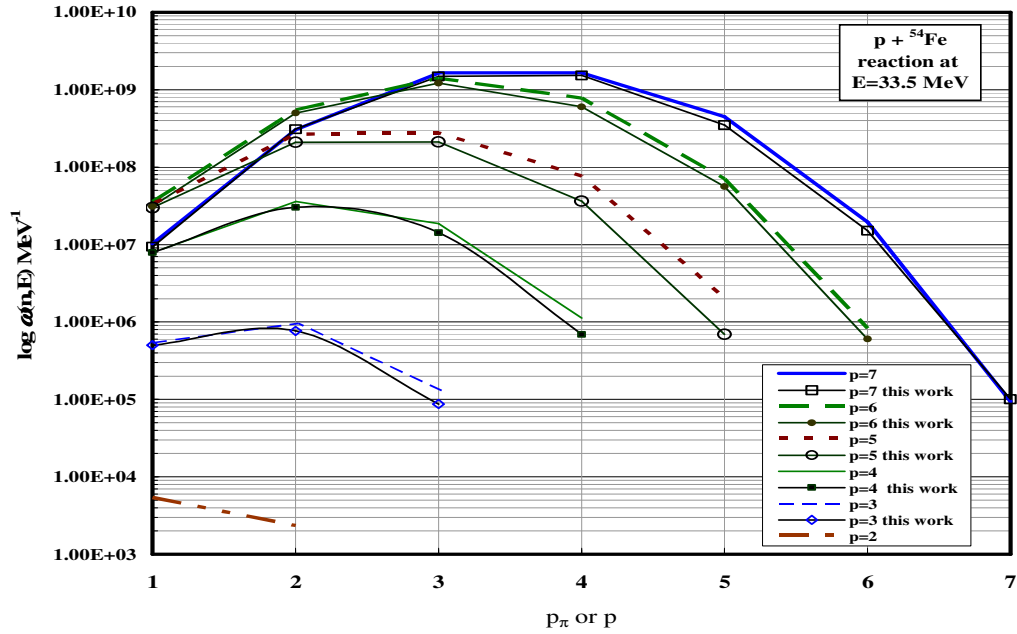


Figure 1: A comparison of the state density results (using Williams' formula) of this work (marked curves) with those of Kalbach [10] (unmarked curves) for  $p+^{54}\text{Fe}$  reaction at 33.5 MeV.

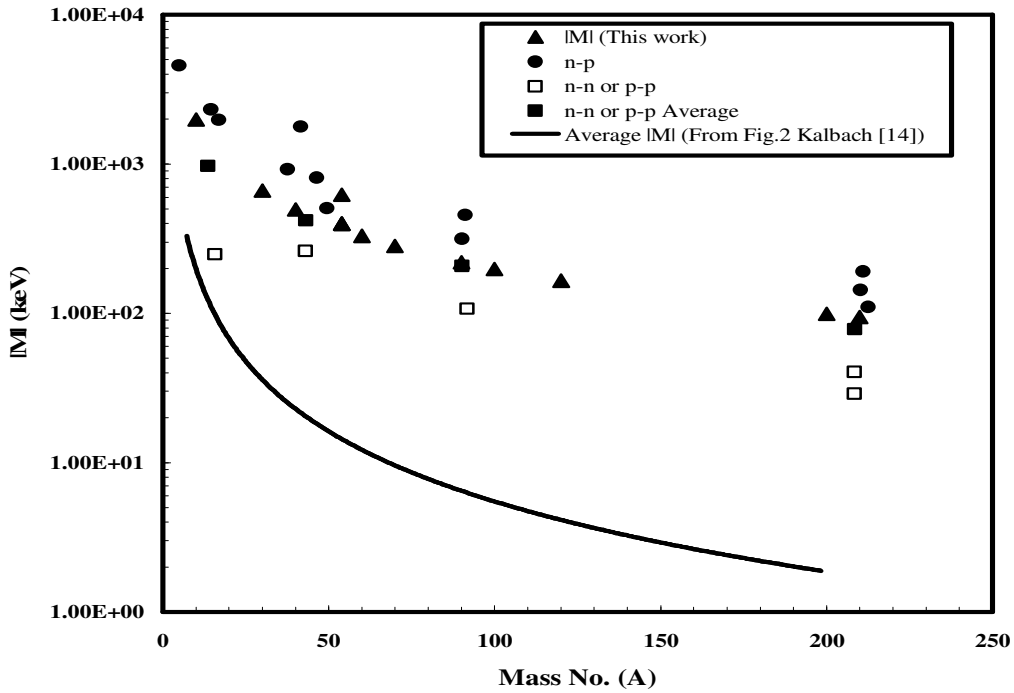


Figure 2: A comparison of the matrix element,  $|MI|$ , used in this work with those of Kalbach[10] for proton reaction with different nuclei at 33.5 MeV.

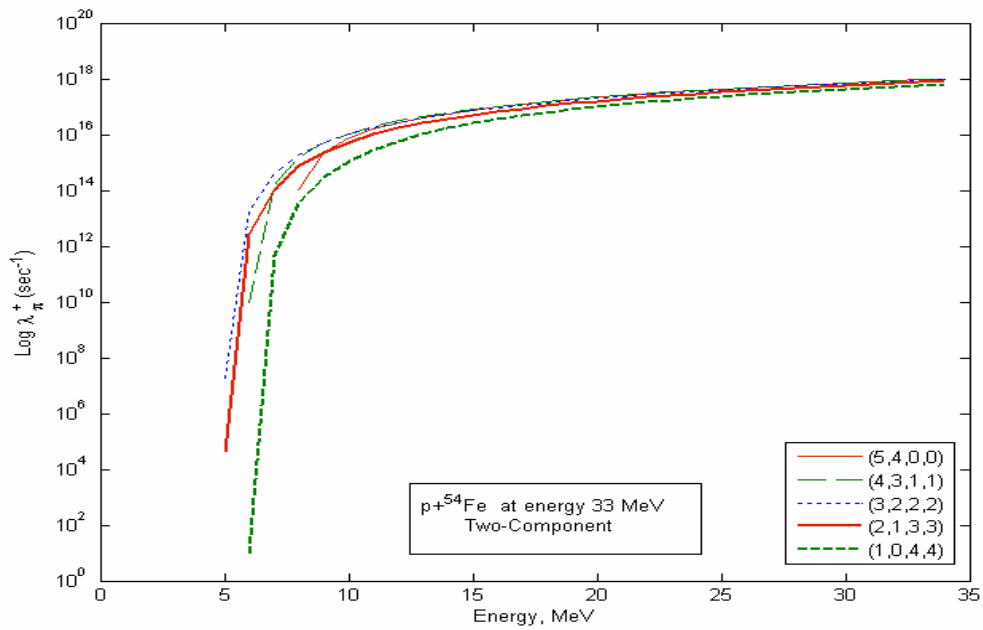


Figure 3-A: The results of the transition rates,  $\lambda_{\pi}^{+}$  calculated in this work as a function of excitation energy for  $p+^{54}\text{Fe}$  reaction at incident energy 33 MeV.  $n_{max}$  is 9.

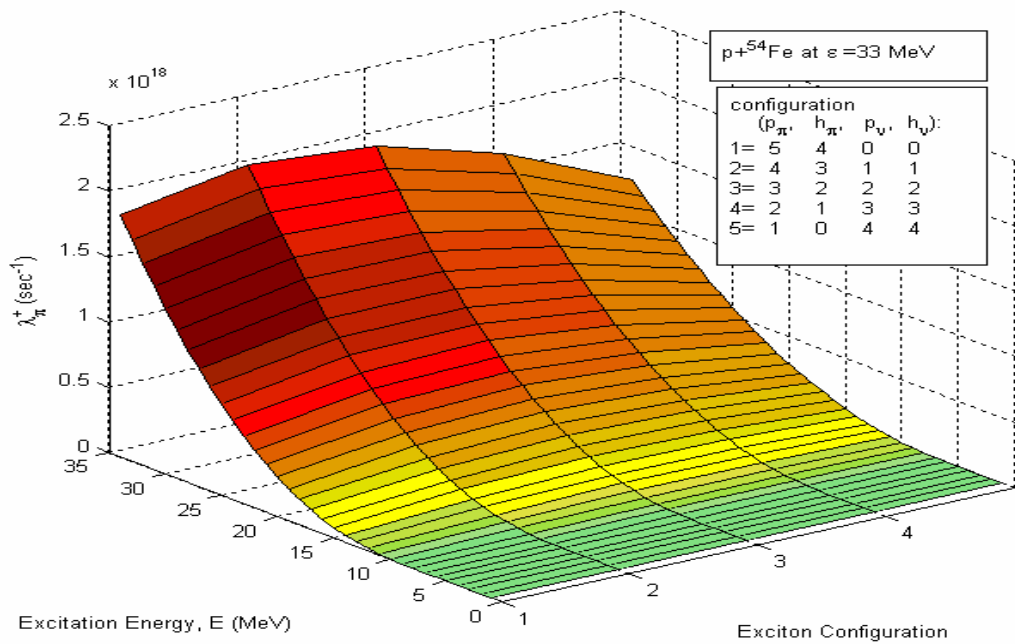


Figure 3-B: The same as Figure 3-A but plotted as a surface.

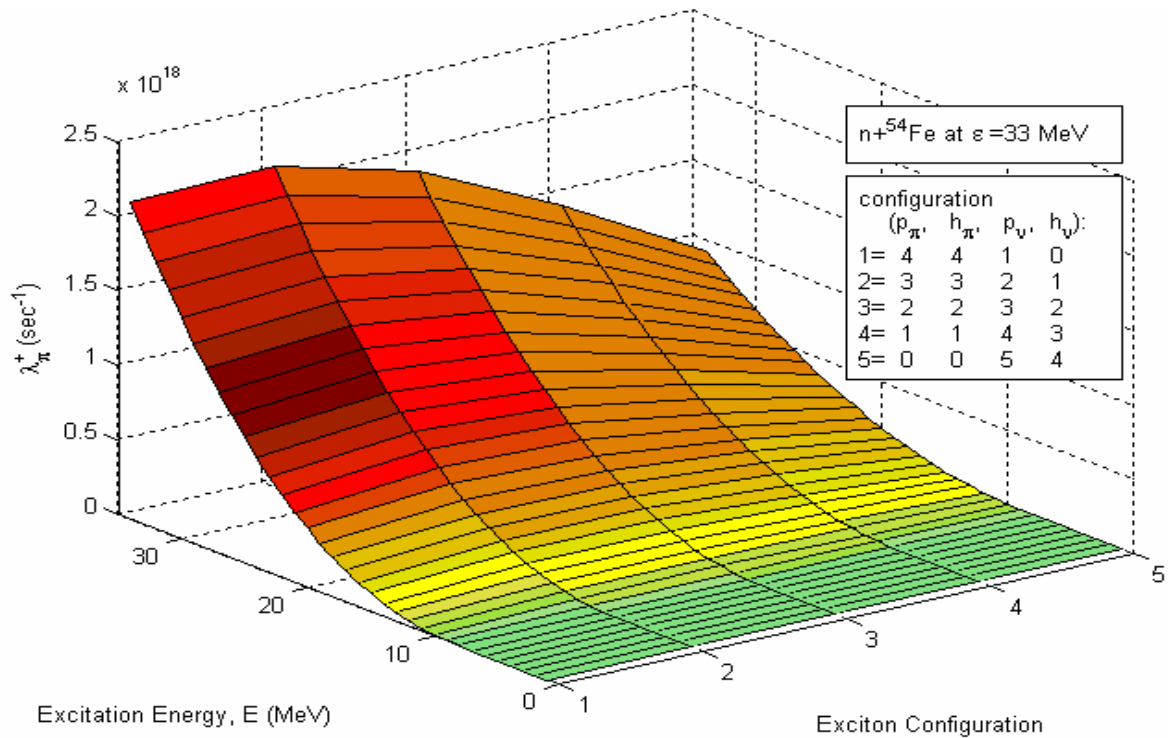


Figure 3-C: The same as Figure 3-B and for n+ <sup>54</sup>Fe reaction at 33 MeV.

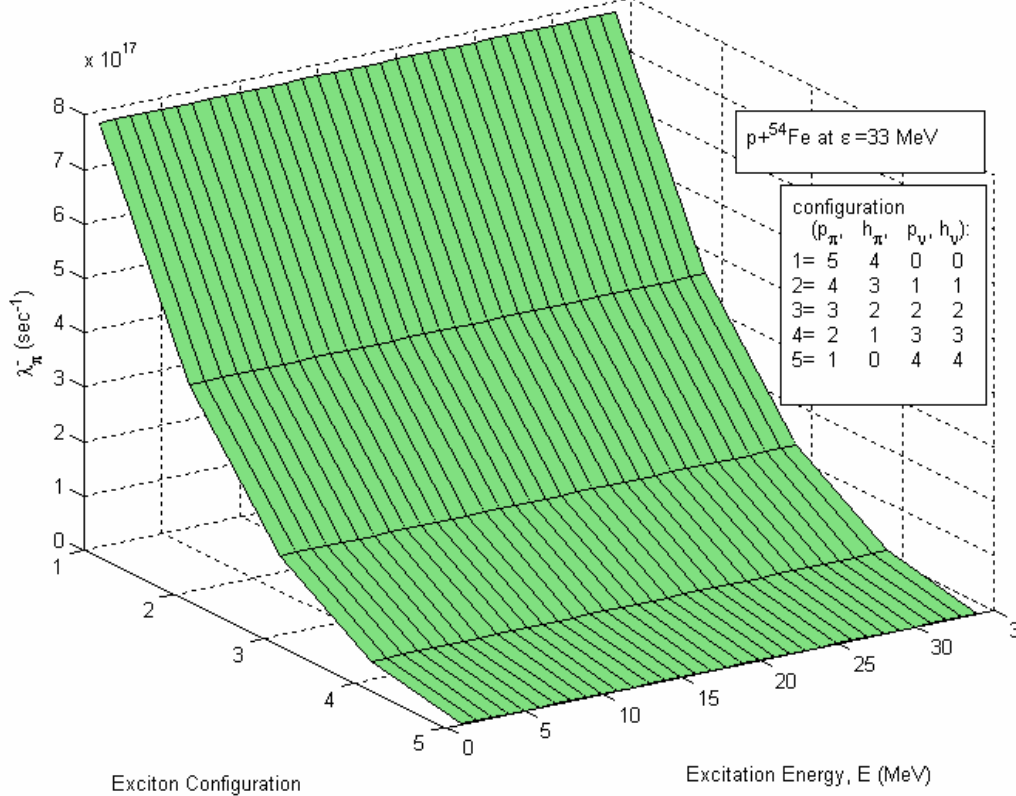


Figure 4-A: The results of the transition rates,  $\lambda_{\pi}^{-}$  calculated in this work as a function of exciton number and excitation energy for p+ <sup>54</sup>Fe reaction at incident energy 33 MeV.

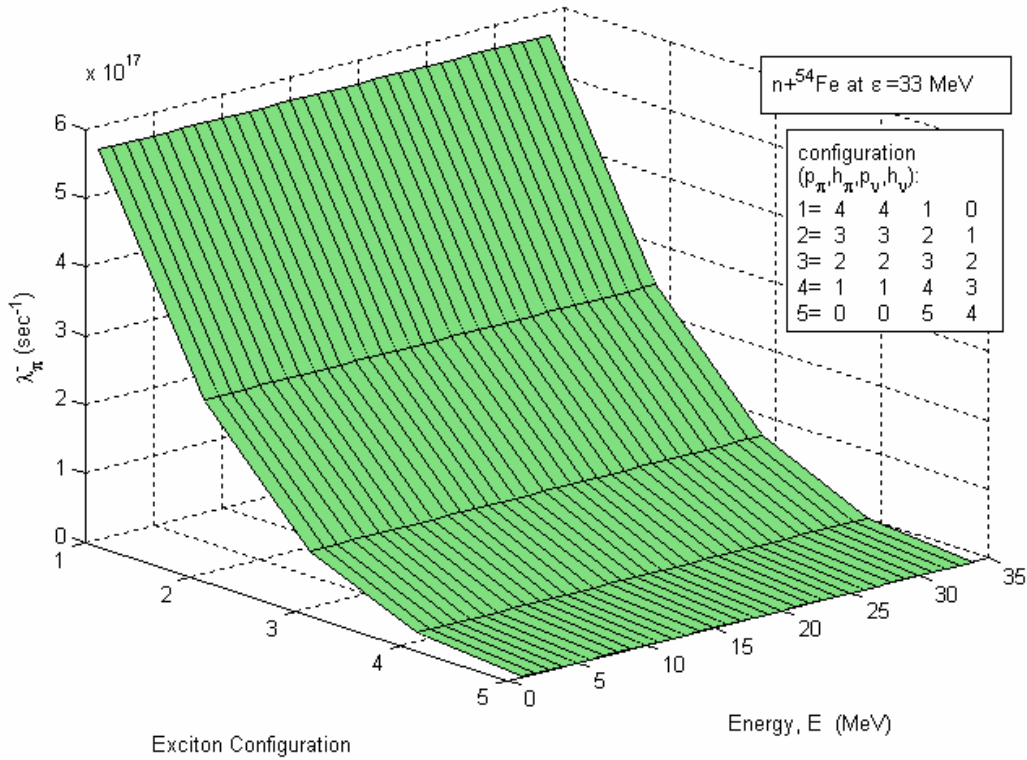


Figure 4-B: The same as Figure 4-A and for n+<sup>54</sup>Fe reaction at 33 MeV.

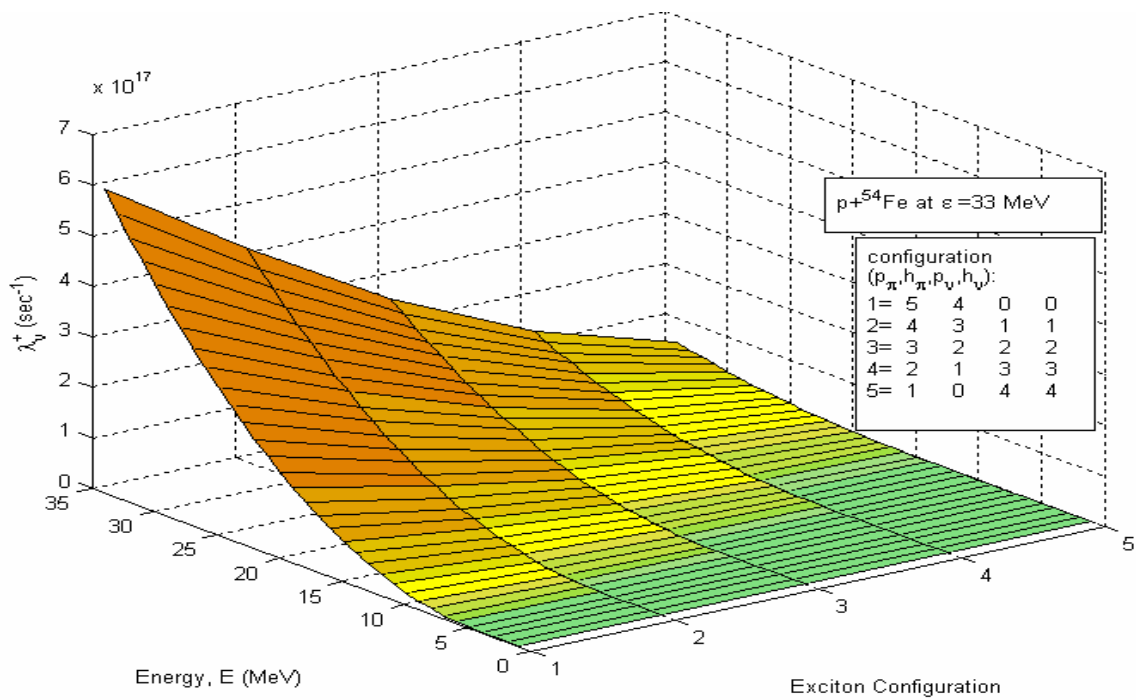


Figure 5-A: The results of the transition rates,  $\lambda_{\nu}^{+}$  calculated in this work as a function of exciton number and excitation energy for p+<sup>54</sup>Fe reaction at incident energy 33 MeV.



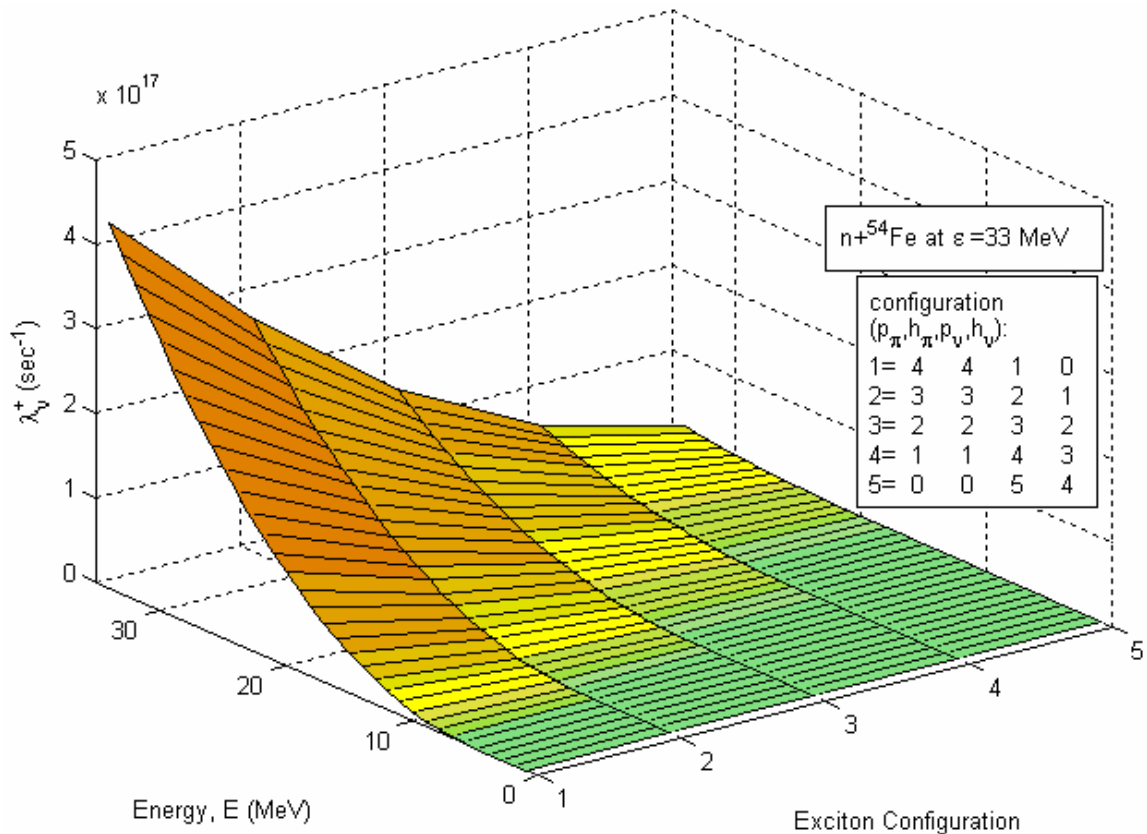


Figure 5-B: The same as Figure 5-A and for n+<sup>54</sup>Fe reaction at 33 MeV.

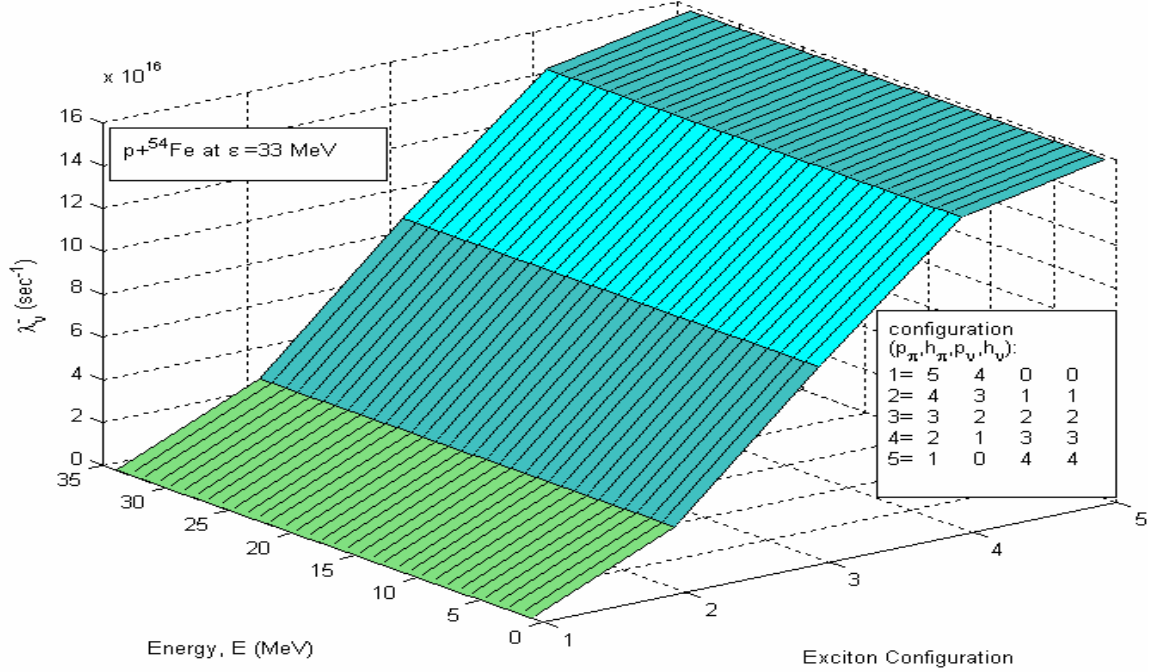


Figure 6-A: The results of the transition rates,  $\lambda_V^-$  calculated in this work as a function of exciton number and excitation energy for p+<sup>54</sup>Fe reaction at incident energy 33 MeV.

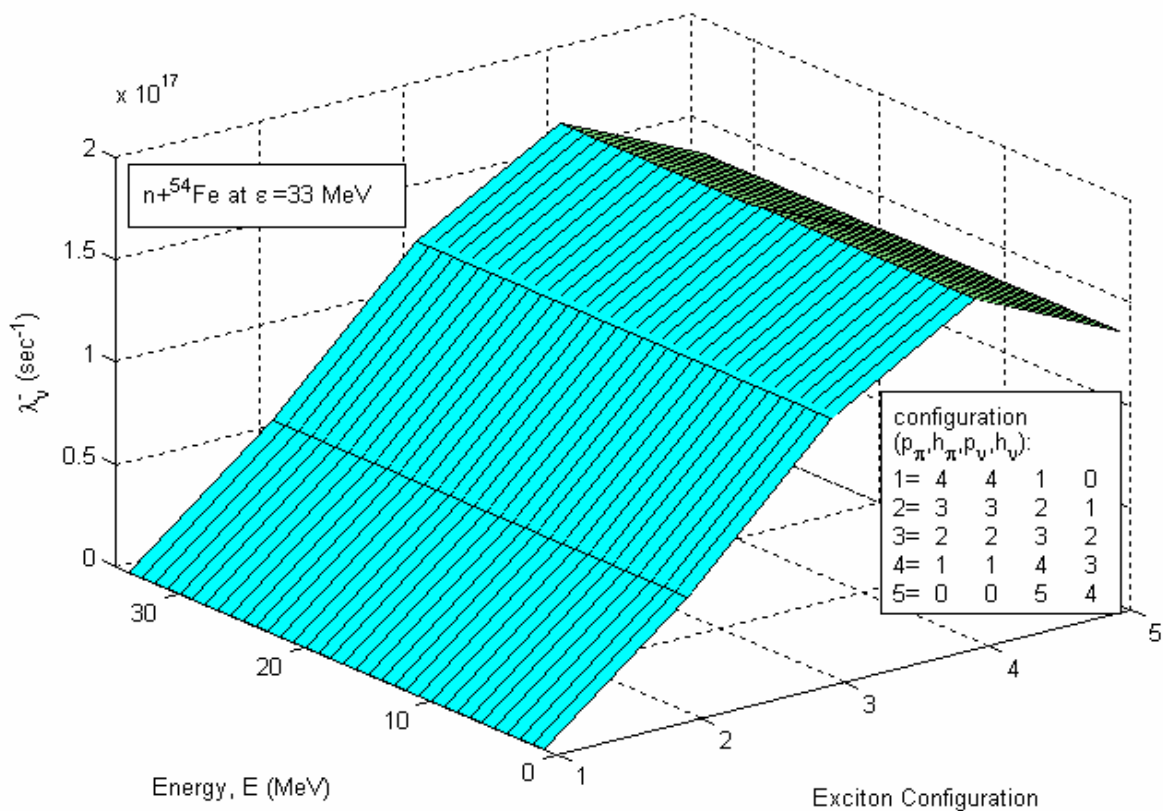


Figure 6-B: The same as Figure 6-A for  $n + {}^{54}\text{Fe}$  reaction at 33 MeV



Figure 7-A: The results of the transition rates,  $\lambda_{\pi\nu}$  calculated in this work as a function of exciton number and excitation energy for  $p + {}^{54}\text{Fe}$  reaction at incident energy 33 MeV.

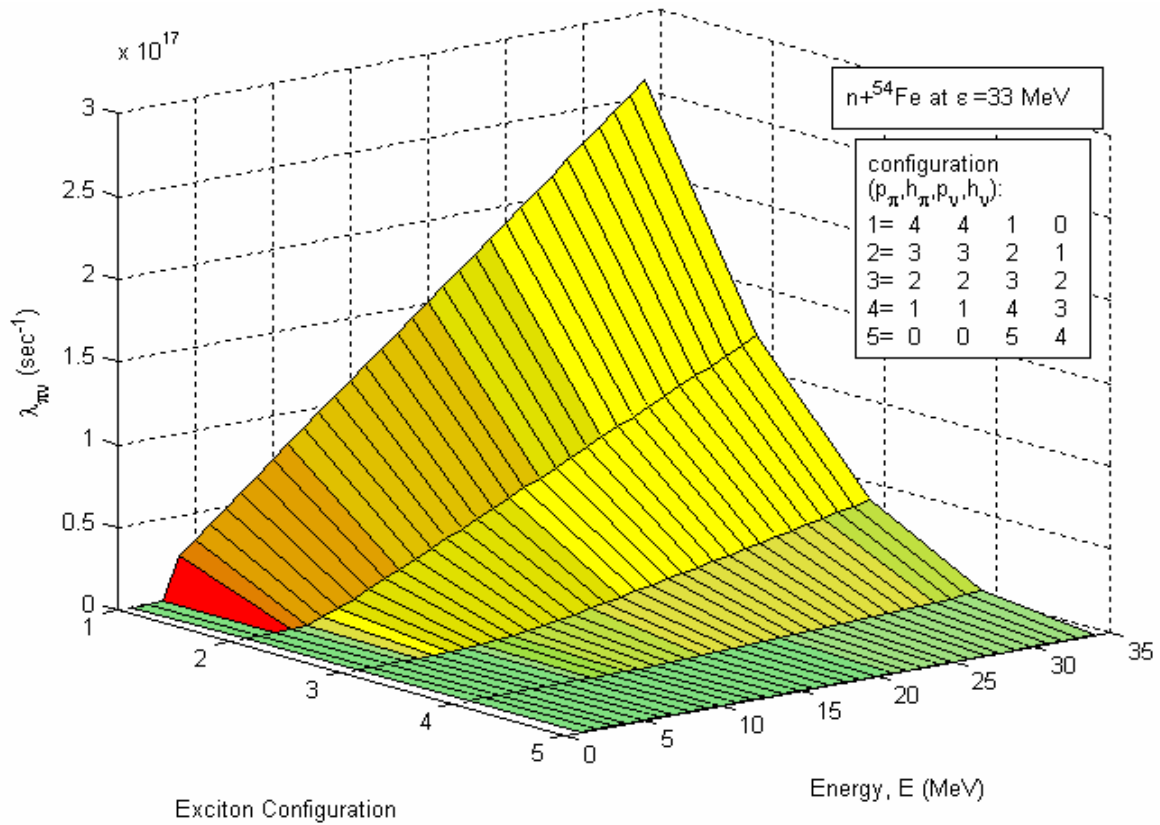


Figure 7-B: The same as Figure 7-A for n+<sup>54</sup>Fe reaction at 33 MeV.

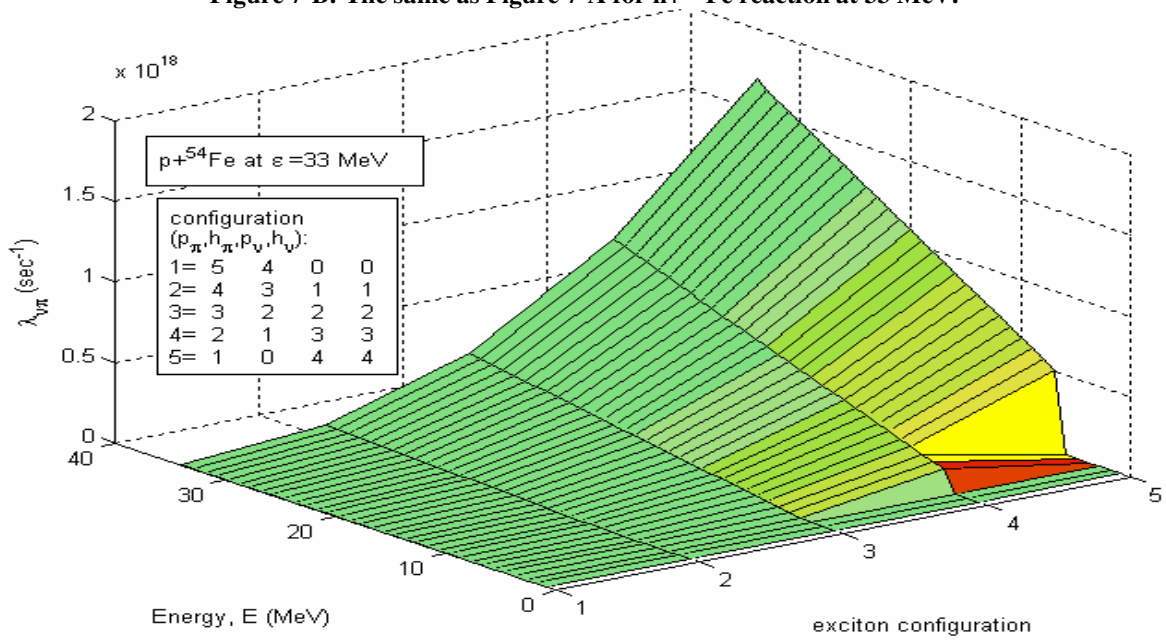


Figure 8-A: The results of the transition rates,  $\lambda_{v\pi}$  calculated in this work as a function of exciton number and excitation energy for p+<sup>54</sup>Fe reaction at incident energy 33 MeV.

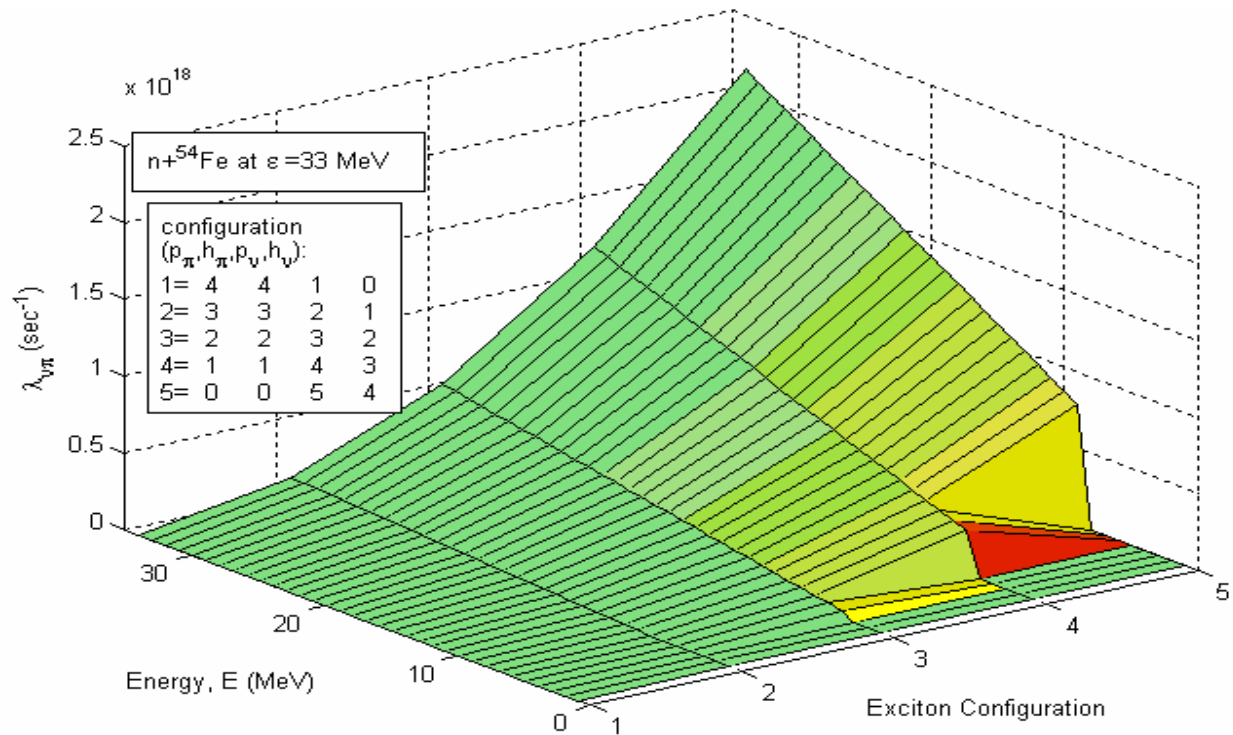


Figure 8-B: The same as Figure 8-A and for n+<sup>54</sup>Fe reaction at 33 MeV

## V. Conclusions

From the above results, one may conclude that neutron and proton induced reactions will differ only by small fraction in the preequilibrium states. This conclusion supports the opinion that the mechanism of development of a nuclear reactions can be explained, to a first degree approximation, as if the incident particle was a (nucleon) only, rather than a neutron or proton. However, this can only be approximate explanation at the first stages of the exciton development, where at higher exciton states with  $n > 3$ , the transitions of the types  $\lambda_{\nu}^{-}$  and  $\lambda_{\pi}^{+}$  differed significantly between neutron and proton transitions.

## References

1. Griffin, J. J., **1966**, Statistical Model of Intermediate Structure, *Phys. Rev. Lett.*, **17**: 478-482.
2. Blann, M., **1968**, Extension of Griffin's Model for Medium-Energy Nuclear Reactions, *Phys. Rev. Lett.*, **18**:1357-1366.
3. Cline, C. K. and Blann, M., **1971**, The Pre-Equilibrium Statistical Model: Description of the Nuclear Equilibration Process and Parameterization of the Model, *Nucl. Phys.* **A172**: 225-247.
4. Sharma, M. K.; Bhardwaj, H. D.; Unnati, G.; Singh, P. P.; Singh, B. P. and Parsad, R. **2007**, Exciton Model Calculations for Alpha-Induced Nuclear Reactions, *Eur. Phys. J.* **A31**: 43-61.
5. Pompeia, C. A. S. and Carlson, B. V. **2007**, Semi-Classical Exciton Model, *Phys. Rev. C* **74**: 054609-054621.
6. Guimarães, F. B.; Fu, C. Y. and Leal L. C., **2002**, Nucleon Induced Reaction Calculations for the Range 5MeV to 2GeV, Oak Ridge National Laboratory Report: ORNL/TM-2001/191-ENDF-366.
7. Hauser, W. and Feshbach, H., **1952**, Inelastic Scattering of Neutrons, *Phys. Rev.* **87**: 366-372.
8. Jasim, M. H.; Shafik, S. S. and Selman, A. A. **2009**, A Suggested Numerical Solution for the Master Equation of the Exciton Model, *J. Kerbala University*, **7 Scientific** (1): 271-282.
9. Selman, A. A. **2009**, Neutron Induced Preequilibrium Nuclear Reactions Using the Exciton Model, Ph.D. Thesis, College

- of Science, University of Baghdad, Baghdad-Iraq.
10. Kalbach, C., **1986**, Two-Component Exciton Model: Basic Formalism Away From Shell Closures, *Phys. Rev.* **C33**: 818-832.
  11. Dobeš, J. and Běták, E., **1983**, Two-Component Exciton Model, *Z. Phys.* **A310**: 329-344.
  12. Kalbach, C., **2007**, Users Manual for PRECO-2006, Exciton Model Preequilibrium Nuclear Reaction Code with Direct Reactions, Triangle Universities Nuclear Laboratory, Duke University, and Kalbach, C., **2005**, Isospin Conversion in Preequilibrium Reactions, *Phys. Rev.* **C72**: 024607-024618.
  13. Williams, F. C., **1971**, Particle-Hole State Density in the Uniform Spacing Model, *Nucl. Phys.* **A166**: 231-249.
  14. Avrigeanu, M. and Avrigeanu, V., **1998**, Partial Level Density for Nuclear Data Calculations, *Comp. Phys. Comm.* **112**: 191-204.

